

Differential effects of human and plant N-acetylglucosaminyltransferase I (GnTI) in plants

Maurice Henquet · Bas Heinrichs · Jan Willem Borst ·
Jochem Eigenhuijsen · Mariëlle Schreuder ·
Dirk Bosch · Alexander van der Krol

Received: 26 February 2009 / Accepted: 27 September 2009
© The Author(s) 2009. This article is published with open access at Springerlink.com

Abstract In plants and animals, the first step in complex type *N*-glycan formation on glycoproteins is catalyzed by *N*-acetylglucosaminyltransferase I (GnTI). We show that the *cgl1-1* mutant of *Arabidopsis*, which lacks GnTI activity, is fully complemented by YFP-labeled plant AtGnTI, but only partially complemented by YFP-labeled human HuGnTI and that this is due to post-transcriptional events. In contrast to AtGnTI-YFP, only low levels of HuGnTI-YFP protein was detected in transgenic plants. In protoplast co-transfection experiments all GnTI-YFP fusion proteins co-localized with a Golgi marker

protein, but only limited co-localization of AtGnTI and HuGnTI in the same plant protoplast. The partial alternative targeting of HuGnTI in plant protoplasts was alleviated by exchanging the membrane-anchor domain with that of AtGnTI, but in stably transformed *cgl1-1* plants this chimeric GnTI still did not lead to full complementation of the *cgl1-1* phenotype. Combined, the results indicate that activity of HuGnTI in plants is limited by a combination of reduced protein stability, alternative protein targeting and possibly to some extend to lower enzymatic performance of the catalytic domain in the plant biochemical environment.

M. Henquet · B. Heinrichs · J. Eigenhuijsen ·
M. Schreuder · A. van der Krol (✉)
Laboratory of Plant Physiology, Wageningen University,
Droevendaalsesteeg 1, 6708 PB Wageningen,
The Netherlands
e-mail: sander.vanderkrol@wur.nl

J. W. Borst
Microspectroscopy Centre, Laboratory of Biochemistry,
Wageningen University, Dreijenlaan 3, 6703 HA
Wageningen, The Netherlands

D. Bosch
Business Unit Bioscience, Plant Research International
BV, Wageningen University and Research Centre,
Droevendaalsesteeg 1, 6700 AA Wageningen,
The Netherlands

D. Bosch
Membrane Enzymology, Department of Chemistry,
Utrecht University, Padualaan 8, 3584 CH Utrecht,
The Netherlands

Keywords *cgl1-1* mutant · GnTI · *N*-glycosylation · Complex glycans

Introduction

In eukaryotes many of the secreted proteins are modified by *N*-glycosylation upon import into the endoplasmatic reticulum (ER). The *N*-glycan biosynthesis starts at the cytoplasmic side of the ER, where sequentially two *N*-acetylglucosamine and five mannose residues are transferred onto the lipid dolichol-P, giving rise to the $\text{Man}_5\text{GlcNAc}_2\text{-PP-Dol}$ intermediate. Then, in a process not well understood, $\text{Man}_5\text{GlcNAc}_2\text{-PP-Dol}$ flips to the luminal side of the ER, where four mannose and three glucose residues are stepwise

added by distinctive glycosyl transferases (Snider et al. 1980; Helenius and Aebi 2002), leading to the lipid-bound precursor oligosaccharide Glc₃Man₉GlcNAc₂. This lipid-linked glycan-moiety is then transferred *en bloc* by the multisubunit oligosaccharyltransferase complex (OST) to the asparagine (N) residues in the consensus N-glycosylation sequence N-X-S/T of nascent protein chains during their translocation into the ER (Kornfeld and Kornfeld 1985). After removal of the three glucose residues and all four α (1,2)-linked mannose residues, the glycan can be further modified by trimming and addition reactions, leading to the so-called complex type glycans.

The first obligatory step in complex type glycans formation in higher eukaryotes, such as plants and animals, is catalyzed by the enzyme *N*-acetylglucosaminyltransferase I (GnTI) (Kornfeld and Kornfeld 1985). Different GnTI genes, originating from animal and plant species have been identified (Kumar et al. 1990; Sarkar et al. 1991; Pownall et al. 1992; Fukada et al. 1994; Puthalakath et al. 1996; Schachter et al. 1997; Strasser et al. 1999; Wenderoth and von Schaewen 2000). All these GnTI genes encode a type II membrane protein, characterized by an N-terminal short cytoplasmic tail, a transmembrane anchor domain, a luminal stem region (combined called the CTS domain) and a luminal catalytic domain at the C-terminus (Kornfeld and Kornfeld 1985). The human GnTI (HuGnTI) has been shown to localize to the medial and trans Golgi in human cell lines (Burke et al. 1994; Grabenhorst and Conradt 1999). In contrast, the GnTI from *N. tabacum* was shown to localise to both the ER and cis-half of the Golgi bodies (Saint-Jore-Dupas et al. 2006).

Previously, an EMS mutant of *Arabidopsis* was identified, which lacks complex glycans due to a point-mutation in *Arabidopsis* GnTI (AtGnTI) (complex-glycan-less: *cgl1-1*; von Schaewen et al. 1993; Strasser et al. 2005). The single point mutation in AtGnTI resulted in a novel N-glycosylation consensus site and a disruption of a highly conserved SQD motif present in all GnTI amino acid sequences characterized so far. This *Arabidopsis cgl1-1* mutant was used for complementation studies by Gomez and Chrispeels (1994), who generated *cgl1-1* calli transformed with the HuGnTI gene. Enzymatic assays of different fractions from a density gradient indicated that both in wild-type and in complemented *cgl1-1* plant cells, human and plant GnTI associated with the fractions which are

typical for Golgi membranes. This indicated that also in plants the HuGnTI localizes to the Golgi system (Gomez and Chrispeels 1994). However, the complementation of the glycosylation defect of *cgl1-1* by HuGnTI was very poor and the total enzyme activity extracted from transformed *cgl1-1* callus was less than 10% of GnTI enzyme activity extracted from wild-type plant cells. Strasser et al. (2005) used a chimeric GnTI construct for complementation of the *cgl1-1* mutant. This construct encodes the rabbit GnTI catalytic domain fused to the CTS region of the plant GnTI. In this case complementation resulted in nearly normal levels of complex *N*-glycans, however it was not investigated if and why there is a difference in complementation efficiency in *Arabidopsis cgl1-1* between plant and mammalian GnTI.

Manipulation of glycosylation in plants with mammalian glycosyltransferases is used for ‘humanizing’ the *N*-glycans on therapeutic proteins that may be produced in plants. However, the activity of mammalian glycosyltransferases in plants is still unpredictable as was the case for expression of human GnTI in the *Arabidopsis cgl1-1* mutant (Gomez and Chrispeels 1994). Also unexpected were the entirely different galactosylated *N*-glycan structures observed when two variants of naturally occurring human galactosyltransferases were expressed in tobacco (Palacpac et al. 1999; Bakker et al. 2001). These observations show that knowledge is lacking to reliably predict the consequences of introducing heterologous glycosyltransferases in plants on *N*-glycosylation. We therefore decided to more thoroughly investigate the differences between expression of the human and *Arabidopsis* GnTI enzyme in plants. We confirmed the low complementation potential of human GnTI in plants and show that a combination of reduced protein stability, reduced catalytic activity and partial alternative sub-cellular targeting, all contribute to the overall low activity of HuGnTI in plants.

Results

Sequence comparison of human and plant GnTI

Comparison of the *Arabidopsis* and human GnTI amino acid sequence shows a low homology at the cytoplasmic, transmembrane and stem region (CTS: 12% sequence identity), but a higher conservation in

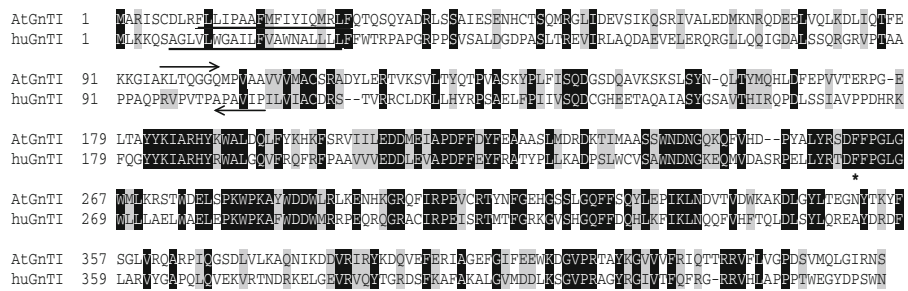


Fig. 1 Alignment of the GnTI protein sequences derived from *Arabidopsis thaliana* (AtGnTI) and human (HuGnTI), using ClustalW. Identical and similar residues are shaded black and grey respectively. The N-glycosylation consensus site of *A.*

thaliana GnTI is indicated with an asterisk and the putative transmembrane regions predicted by HMMTOP v2 are underlined. The position of primers used for the construction of the chimeric plant-human GnTI, are indicated with an arrow

the catalytic domain (38% sequence identity) (Fig. 1). In contrast to the mammalian GnTIs, which do not have an N-glycosylation site, the plant GnTI sequences identified to date contain one putative N-glycosylation site. However, the location of the N-glycosylation site in tobacco and potato GnTI differs from that in *Arabidopsis* GnTI (Wenderoth and von Schaewen 2000). The hydrophobic transmembrane anchor domain of plant and human GnTI predicted by HMMTOP V2 (Tusnady and Simon 2001), is at the same relative position, but the transmembrane domain for the human GnTI is predicted to be slightly larger. The size of the transmembrane domain may be of influence for the sub-cellular localization of the protein, as indications (from mammalian cells) are that membrane thickness increases from ER to Golgi (Grabenhorst and Conradt 1999; Brandizzi et al. 2002; Neumann et al. 2003; Saint-Jore-Dupas et al. 2006). In addition, analysis of the HuGnTI and AtGnTI signal peptide sequences in the plant version of SignalP showed a probability of 0,068 for signal peptide cleavage of AtGnTI (position 26) and a probability of 0,472 for signal peptide cleavage of the HuGnTI (position 35). Cleavage of mammalian GnTI in a heterologous host was indeed demonstrated for the rat GnTI (SignalP probability 0,229 at position 35) in *Saccharomyces cerevisiae* cells (Yoshida et al. 1999).

Different levels of complementation in the *cgl1-1* lines with plant, human or chimeric GnTI

Expression constructs were made with the HuGnTI or AtGnTI gene and a Chimeric GnTI (ChGnTI) gene, encoding the *Arabidopsis* CTS domain (amino acid

residues 1–102) and the human catalytic domain (amino acid residues 102–445). At the 3' end, the GnTI coding sequences were fused in frame to the coding sequence of fluorescence marker sequences (YFP or CFP), to facilitate detection in plant cells. The coding sequences were put under control of the Cauliflower Mosaic Virus 35S promoter in the binary vector pBinplus (van Engelen et al. 1995) and *Arabidopsis cgl1-1* mutant plants were transformed using the *Agrobacterium tumefaciens* floral dip method (Clough and Bent 1998). Transgenic plants were selected by germinating seeds on medium containing kanamycin, which yielded for each construct at least nine independently transformed plants.

First, the average level of functional complementation in each set of transformants was determined. Proteins extracted from individual primary transformants and wild-type plants were probed in an Elisa assay with serum directed at plant complex glycans, to determine the level of complementation towards proteins with complex type glycans in each line. The results show that the average level of proteins with complex glycans was similar to wild-type in the *cgl1-1* plants expressing the AtGnTI-YFP (AtGnTI^{cgl1}) or ChGnTI-YFP (ChGnTI^{cgl1}), but low in *cgl1-1* plants expressing the HuGnTI-YFP (HuGnTI^{cgl1}) (Fig. 2).

From each set of transformants, plants with a single locus insert were identified by segregation analysis of T2 seedlings on medium containing kanamycin. For each of the constructs three independent single-locus-insert homozygous lines were developed, with highest, intermediate and with low level of complementation. Progeny seedlings from these homozygous lines were analyzed for levels of glycoproteins modified with complex glycans, both by western blots analysis and by

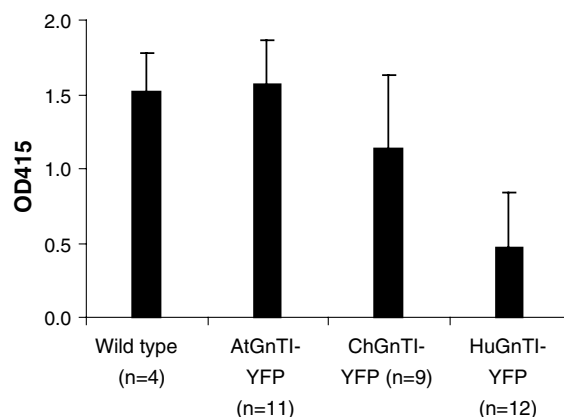


Fig. 2 Complementation of *cgl1-1* plants. Proteins extracted from primary T1 transformants from AtGnTI-YFP^{cgl}, ChGnTI-YFP^{cgl}, HuGnTI-YFP^{cgl} and wild type plants were probed in an Elisa assay with serum directed at plant complex glycans. Error bars represent SD

Elisa (Fig. 3a, b). The results from the western blots show no specific qualitative differences in the patterns of proteins labeled with complex glycans and therefore glycosylation levels only differ quantitatively between the lines (Fig. 3a). In the ChGnTI^{cgl} lines the highest signal was slightly lower than of the highest in the AtGnTI^{cgl} lines, but in all three the HuGnTI^{cgl} plants the level of proteins with complex glycans was very low (Fig. 3b).

Relating transgene expression level to *cgl1-1* complementation

To relate the level of complementation in the different homozygous transgenic lines to the mRNA expression level of the transgene, RNA isolated from the selected lines was analyzed with real-time semi-quantitative RT-PCR, using YFP-specific primers and actin as an internal control. The results show a comparable level of transgene expression in the three AtGnTI^{cgl} lines and two of the ChGnTI^{cgl} lines (Fig. 4a). In ChGnTI^{cgl} line 6 the expression level of the transgene was higher than in any of the other lines (Fig. 4a), while in all three HuGnTI^{cgl} lines the expression was higher than in the three AtGnTI^{cgl} lines. Nevertheless, complementation in the three HuGnTI^{cgl} lines was lower than in the AtGnTI^{cgl} lines (Fig. 3) indicating that mRNA levels are not limiting complementation by the HuGnTI gene.

Lines carrying the *Arabidopsis*, chimeric and human GnTI-YFP fusion constructs with similar

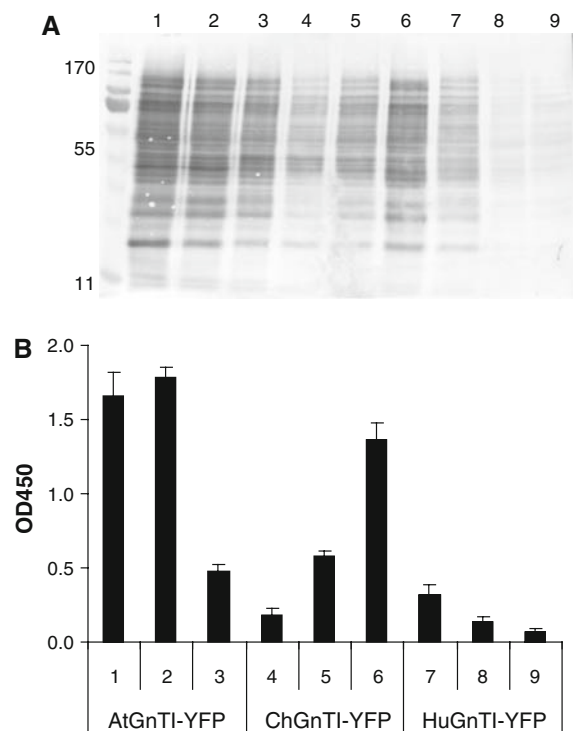


Fig. 3 Complementation of *cgl1-1* complemented plants. Selected AtGnTI-YFP^{cgl} (lane 1–3), ChGnTI-YFP^{cgl} (lane 4–6) and HuGnTI-YFP^{cgl} (lane 7–9) T2 lines were analyzed by immunoblotting (**a**) or Elisa (**b**) using a polyclonal anti-HRP antibody that specifically recognizes complex type N-glycans. Molecular weight markers are indicated on the left. Error bars represent SD

mRNA expression levels (Fig. 4a: samples 1, 5 and 8) and lines with the highest mRNA expression level (Fig. 4a: samples 1, 6 and 7) were used to relate the mRNA level to the ectopically produced GnTI-YFP fusion protein level and the level of complementation. Protein extracts were probed on a Western blot with antibodies directed against YFP (Fig. 4b). In the *cgl1-1* lines transformed with AtGnTI-YFP (sample 1) and ChGnTI-YFP (sample 5 and 6) a band of 78 kDa was detected, corresponding to the mass of the GnTI-YFP fusion protein. However, the GnTI-YFP protein fusion product was not detected in protein extracts from the two HuGnTI^{cgl} lines (Fig. 4b), even though a low level of complementation was observed in these plants (Fig. 3, lane 7–9). This shows that HuGnTI-YFP protein is active in these plants, but accumulates at relatively low levels. In all extracts a protein fragment of ~27 kDa was detected, corresponding to free YFP, indicating that

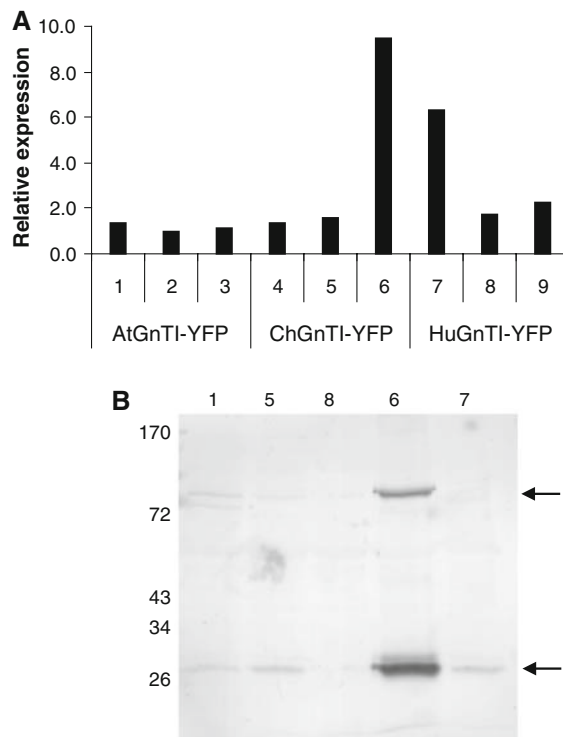


Fig. 4 GnTI-YFP expression in transgenic *cgl1-1* lines. **a** Quantification of the amount YFP transcript using real-time PCR (black bars) in pooled seedlings of selected AtGnTI-YFP^{cgl} (1–3), ChGnTI-YFP^{cgl} (4–6) and HuGnTI-YFP^{cgl} (7–9) lines. The RT-PCR results are expressed as the ratio between the amounts of YFP versus the amount of actin transcript. **b** Immunoblotting using monoclonal anti-GFP antibodies in transgenic lines. The upper arrow indicates the position of the GnTI-YFP fusion protein and the lower arrow indicates the position of cleaved free YFP. Molecular weight markers are indicated on the left

the fusion of the proteins with YFP is prone to proteolytic cleavage.

When free YFP is cleaved from the GnTI-YFP fusion proteins, the remainder of the membrane bound GnTI protein may still contribute to GnTI activity in cells. Therefore, the combined signal from full length GnTI-YFP protein and the free YFP protein band can be taken as a measure for the total ectopic protein expression level. This combined signal is similar for HuGnTI-YFP^{cgl} (sample 7) and AtGnTI^{cgl} (sample 1), despite the approximately five-fold difference in transgene mRNA levels in these lines (Fig. 4a). In addition, the similar level of ectopically produced protein in HuGnTI-YFP^{cgl} and AtGnTI-YFP^{cgl} did not result in similar levels of complementation (Fig. 3). The combined signal from

HuGnTI-YFP and free YFP was strongest in sample 6 (HuGnTI-YFP), consistent with the very high transgene mRNA expression level in this line. However, complementation level in this line was not as high as in the *cgl1-1* lines with homologous (AtGnTI) complementation, indicating that the catalytic domain of HuGnTI may be less active in plants.

Sub-cellular localization of the GnTI-YFP fusion protein

We analyzed the sub-cellular localization of the different GnTI-YFP fusion proteins in cells of leaves from 10-day old transgenic seedlings by whole mount confocal microscopy. As could be expected from the expression levels in leaves, the YFP fluorescence signal was most clearly detected in leaves of *cgl1-1* seedlings transformed with AtGnTI-YFP or ChGnTI-YFP. The YFP fluorescence in these plants displayed a punctuated pattern, consistent with a Golgi-localization of the fusion protein (Fig. 5). No fluorescence signal above background levels were detected in leaves of *cgl1-1* plants complemented with HuGnTI (Fig. 5), consistent with the lack of detection on western blot of intact HuGnTI-YFP fusion protein in these plants (Fig. 4). The low fluorescence signal in the stably transformed plants with HuGnTI-YFP prevented accurate sub-cellular localization of the gene product(s). Therefore, to confirm that the HuGnTI-YFP expression construct can produce intact fusion protein in plants and to obtain a better signal for sub-cellular localization of this fusion protein in plant cells, a transient protoplast expression assay was used.

The plant, human or chimeric GnTI protein were fused to both YFP and CFP and the different expression constructs were pair wise introduced into *Arabidopsis* protoplasts through transfection. At 24 h post-transfection the sub-cellular localization of the resulting YFP and CFP fluorescence signal was determined using confocal laser scanning microscopy (CLSM). In addition, to confirm the putative Golgi localization, co-localization experiments were performed with the different GnTI-CFP fusion proteins and the established (trans)Golgi marker STtmd-YFP (Grebe et al. 2003).

Transient co-expression of the individual GnTI-CFP expression constructs with the YFP-labeled Golgi marker in *Arabidopsis* protoplasts showed a distinct CFP signal, which localized to Golgi-like

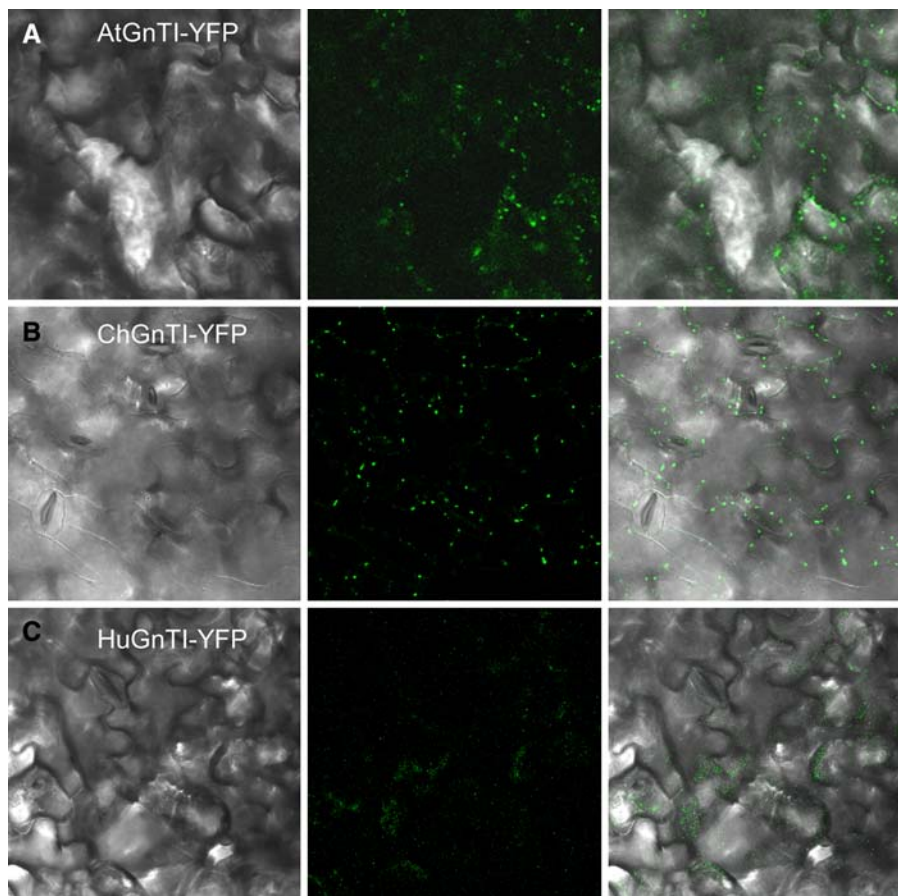


Fig. 5 Localization of the GnTI-YFP fusion proteins in leaves of 10 day old transgenic T2 seedlings by whole mount microscopy. *Left:* light images leaf surface. *Middle:* fluorescent images taken under equal filter and exposure settings. *Right:* overlay light and fluorescent images. Seedlings expressing AtGnTI-YFP or ChGnTI-YFP, displayed a punctate

fluorescence pattern consistent with a Golgi-localization. In seedlings expressing HuGnTI-YFP either no or only very weak punctuated fluorescence was detected. Similar results were obtained for at least three independent transformed lines expressing the different constructs

compartments for all fusion proteins, including HuGnTI-CFP (Fig. 6, CFP signal).

The fluorescence signal from HuGnTI in protoplasts indicates that, contrary to stably transformed plants, the conditions of the transient expression assay do allow the detection of this protein in plant cells. Indeed, intact HuGnTI fusion protein in protoplasts could now be detected by western blot analysis (Fig. 7, lane 3). Results also show that the ~27 kDa protein band representing free YFP/CFP, is mostly present in the medium fraction, indicating that cleaved YFP/CFP is mostly secreted (Fig. 7, lane 4). In protoplasts transfected with the AtGnTI-CFP and STtmd-YFP, both full length fusion proteins are detected in the protoplast fraction, while free CFP

(and/or YFP) was again detected in the medium fraction (Fig. 7, lane 2).

All GnTI-YFP fusion proteins showed a similar and high degree of co-localization with the Golgi marker in the transfection assay (Fig. 6). Also, when fluorescently labeled AtGnTI and ChGnTI were co-expressed, the protein products showed a high degree of co-localization (Fig. 8). However, when protoplasts were co-transfected with the AtGnTI-CFP and the HuGnTI-YFP expression constructs together, the CFP and YFP signal showed a lower degree of co-localization to the same Golgi stacks: in addition to double-labeled Golgi stacks, also Golgi stacks labeled by only AtGnTI-CFP, as well as Golgi stacks only labeled by the HuGnTI-YFP fusion protein were

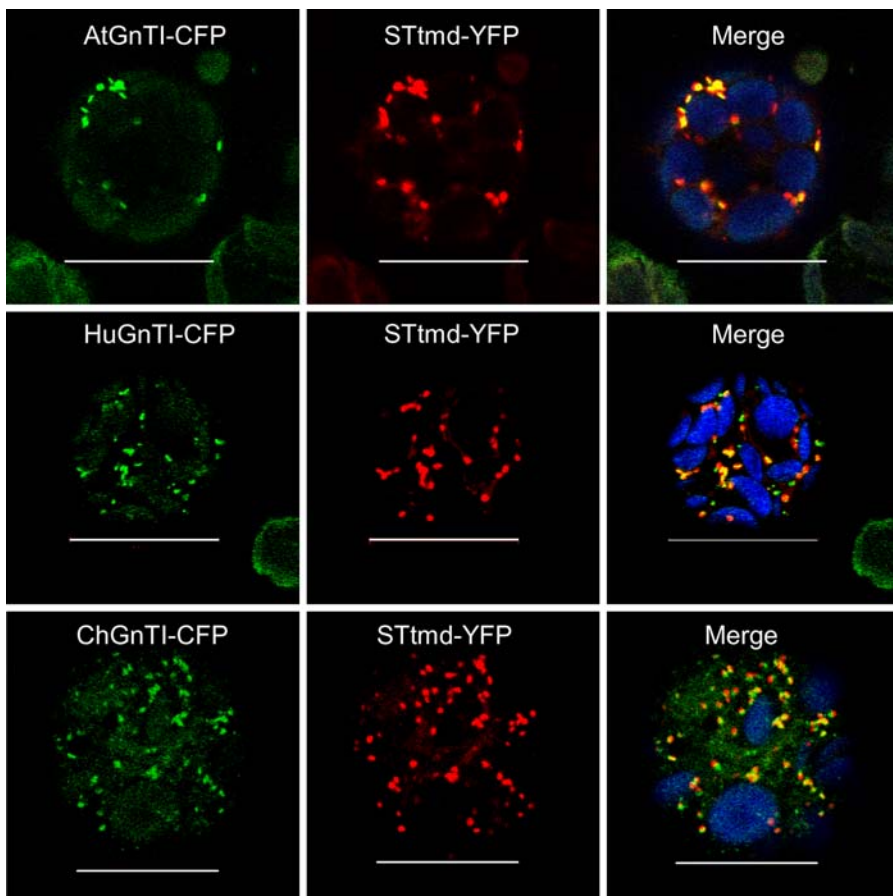


Fig. 6 Co-localization of the GnTI-CFP fusion proteins with the STtmd-YFP Golgi marker in wild-type *A. thaliana* protoplasts by confocal laser scanning microscopy. *Left column* represents different constructs showing the CFP signal; *middle column*: fluorescence of STtmd-YFP construct; *right column*:

overlay of both staining patterns (*green*: CFP; *red*: YFP; *yellow*: overlay CFP/YFP; *blue*: chlorophyll). The distinct fluorescence signal from YFP and CFP in the protoplasts showed good co-localization. *White bar* represents 20 μ m. (Color figure online)

detected (Fig. 8). Similar results were obtained in transfection experiments when reciprocal labeled fusion constructs (AtGnTI-YFP and HuGnTI-CFP) were used. In contrast to when HuGnTI was transfected alone, we noted that in many experiments the fluorescence signal from the HuGnTI was low, or not even detectable, when in the transfection the HuGnTI was co-expressed with the AtGnTI, regardless of the CFP or YFP fluorescent label. Therefore, only experiments in which protoplasts gave a clear dual labeling were included in the score. Reduced fluorescence signal due to lower HuGnTI accumulation could lead to an overestimation of Golgi stacks only labeled by AtGnTI fusion protein. However, also Golgi stacks in the protoplasts are labeled only by the HuGnTI, suggesting a sub-cellular localization that is

partly distinct from the sub-cellular localization of AtGnTI in these transfection experiments.

Discussion

Multiple reasons for low complementation efficiency of plant *cglI-1* by HuGnTI

Expression of heterologous glycosyltransferases in plants is used to manipulate *N*-glycans on target glycoproteins to advance the use of plants as production platforms of therapeutic proteins. However, the factors that determine optimal activity of heterologous enzymes within the context of the endogenous plant glycosylation pathway are not well

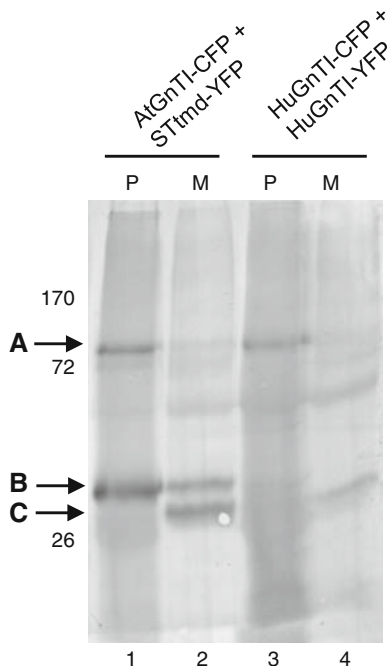


Fig. 7 Western blot analysis of protoplasts from two separate co-transfections. Proteins were extracted from the protoplast (p) and the medium (m) from a co-transfection assay with the plant GnTI-CFP and the YFP-Golgi marker (lane 1 and 2) and a co-transfection with HuGnTI-YFP and HuGnTI-CFP (lane 3 and 4) and used for western blotting with antibodies against GFP. The position of the GnTI fusion proteins (**a**), the YFP-Golgi marker (**b**) and the free cleaved YFP/CFP (**c**) is indicated by the arrows on the left. Molecular weight markers are indicated on the left

understood. Efficient expression of heterologous glycosyltransferases depends not only on efficient transcription and translation but also on their proteolytic stability and sub-Golgi localization in the new host and possibly on interactions with other endogenous components of the glycosylation machinery of the host. Here we have investigated with respect to several characteristics the expression of human GnTI in plants, which in previous experiments was shown to have only limited activity in plant calli (Gomez and Chrispeels 1994).

The activity of plant and human GnTI was compared in a complementation assay using transgenic lines of the *Arabidopsis* mutant *cgl1-1* (Figs. 2 and 3). The results confirm the low complementation potential of the human GnTI gene in plants, as previously shown by Gomez and Chrispeels (1994), however, in their case the complementation potential of human GnTI gene in *Arabidopsis* was not directly

related to expression and activity of the wild-type *Arabidopsis* GnTI gene. Comparison of the mRNA expression levels and the complementation potential of fluorescently tagged AtGnTI, HuGnTI and ChGnTI variants showed that all genes are well transcribed and that the low complementation by HuGnTI must be due to post-transcriptional limitations.

When lines with equal transgene mRNA steady state level are compared (Fig. 4a, lanes 1, 5 and 8), the Western blot analysis shows that the plant and chimeric fusion protein product levels are very similar, but from the HuGnTI-YFP protein no product, neither fusion nor free YFP is detected. This indicates a reduced stability of the HuGnTI-YFP protein in plants and probably a reduced translation of the HuGnTI-YFP mRNAs. Indeed, an approximately 6-fold higher transgene mRNA steady state level was required (Fig. 4a, lane 1 and 7) to get similar levels of ectopically produced protein products in the AtGnTI-YFP^{cgl1} and HuGnTI-YFP^{cgl1} plants, as indicated by the combined signal of the fusion protein and free YFP (Fig. 4b, lane 1 and 7). However, this did not result in equal levels of complementation of the complex glycan levels in these lines (Fig. 3a, lane 1 and 7).

When the CTS domain of HuGnTI was replaced by the AtGnTI CTS domain the average complementation level in 9 independent transformants was almost equal to that of the lines transformed with the plant GnTI (Fig. 2). However, when lines with equal expression levels were compared (Fig. 4a, lane 1 and 5), complementation efficiency of the ChGnTI-YFP was shown to be significantly higher than with HuGnTI-YFP but not as high as that of AtGnTI-YFP (Fig. 3, lanes 1 and 5). Even though ChGnTI-YFP and AtGnTI-YFP were targeted with high degree to the same sub-cellular compartments (Fig. 6), the catalytic domain of HuGnTI is apparently enzymatically not as active in plants as that of plant GnTI. Because the sequence of human and chimeric mRNA is very similar (83% identical) and have identical 5' untranslated sequences, we assume a similar translational efficiency of these two mRNA's in plants. As equal ChGnTI and AtGnTI mRNA steady state levels resulted in equal protein steady state levels, we therefore assume that HuGnTI mRNA is as efficiently translated in plants as AtGnTI mRNA and the reduced activity of HuGnTI is therefore ascribed to post-translational characteristics

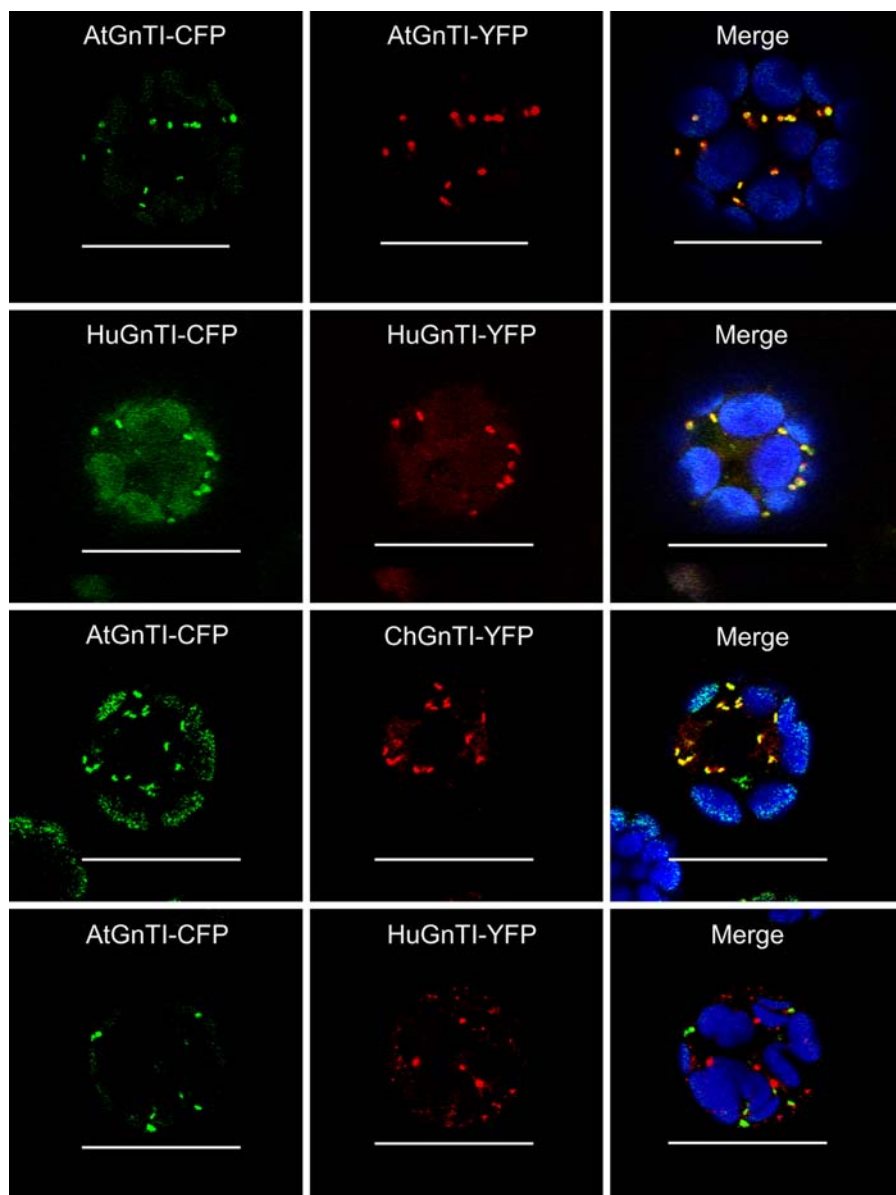


Fig. 8 Co-localization of the AtGnTI or/and the HuGnTI fusion protein with either the YFP and CFP marker in wild-type *A. thaliana* protoplasts by confocal laser scanning microscopy. *Left column*: represents constructs showing the CFP signal, *middle column*: fluorescence of GnTI-YFP construct, *right column*: overlay of both staining patterns (yellow color indicates overlay) combined with the chlorophyll signal (blue color). White bar represents 20 μ m. (Color figure online)

column: fluorescence of GnTI-YFP construct, right column: overlay of both staining patterns (yellow color indicates overlay) combined with the chlorophyll signal (blue color). White bar represents 20 μ m. (Color figure online)

such as the apparent reduced protein stability, mis-targeting or reduced activity of the catalytic domain of HuGnTI.

A factor which may contribute to the instability of HuGnTI protein in plants is the relatively high score for cleavage of the transmembrane anchor according to the signal peptide sequence prediction. Cleavage of the transmembrane anchor would result in a soluble

form of HuGnTI-YFP, which may not be retained efficiently in the Golgi.

Subcellular localization of plant, chimeric and human GnTI

Localization studies in stably transformed plants showed a clear punctuate fluorescence signal in the

ChGnTI^{cg1} and AtGnTI^{cg1} lines, indicative of Golgi localization. However, no apparent Golgi-localized YFP signal was detected in transgenic plants expressing HuGnTI-YFP (Fig. 5). We reasoned that in a transient expression assay like with plant protoplasts, the transient expression pulse from the high copy number of the introduced expression vector, combined with reduced protein degradation in protoplasts, may be sufficient to allow for detection of the HuGnTI-YFP fusion product. Indeed, transfection with the HuGnTI-YFP expression construct resulted in a clear fluorescence signal localized to distinct Golgi stacks, which were demonstrated to be Golgi stacks by co-transfection with a marker protein (Fig. 6). In addition, also the full length HuGnTI-YFP protein was now detected in protoplast protein extracts by western blotting, while in the medium a fraction of free YFP was detected (Fig. 7).

We used co-localization studies to determine if AtGnTI and HuGnTI target the same subcellular compartments in plant cells. In our experimental set-up, co-localization studies can clearly distinguish between cytosolic, ER and Golgi stacks, but not between individual cisternae. When identical GnTI proteins, fused to either YFP or CFP, were co-expressed in protoplasts, a high degree of co-localization to the same Golgi stacks was observed (Fig. 8), indicating that the relatively high gene dosage that is used in the protoplast transfection assays does not lead to alternative targeting of differentially labeled proteins per se. Indeed, also when fluorescently labeled AtGnTI and ChGnTI were co-expressed, the protein products showed a high degree of co-localization (Fig. 8). In contrast, when AtGnTI-YFP and HuGnTI-CFP were co-expressed in the same protoplasts (using the same gene dosage in the transfection), limited co-localization of these two different forms of the GnTI was observed (Fig. 8). Moreover, similar results were obtained when reciprocally labeled proteins were used for the AtGnTI/ChGnTI and AtGnTI/HuGnTI co-localization studies (data not shown). We noted that the signal from the fluorescently labeled HuGnTI was consistently low when expressed together with the plant GnTI fusion protein, but not when co-expressed with the Golgi marker or with reciprocally labeled HuGnTI. It has been reported that plant cells appear to have a high flexibility in using the ER to assemble novel organelles (Lisenbee et al. 2003; Masclaux et al. 2005)

which could be related to the partial unique localization of HuGnTI in the protoplast transient expression assay. If and how this further relates to the reduced complementation activity of HuGnTI in stably transformed plants would require additional experiments with new transgenic lines with sufficiently high expression and high resolution (electro-)microscopical studies.

In summary, our results show that the low complementation capacity of the human GnTI is caused by post-transcriptional limitations. The low activity of HuGnTI in plant cells can thus be explained by reduced stability of HuGnTI protein compared to plant GnTI, including cleavage of the catalytic domain from the membrane anchor and possibly by a potential of HuGnTI to target Golgi stacks other than those targeted by AtGnTI. The data obtained with ChGnTI show that these differences can be ascribed to differences in the CTS region and in addition that the catalytic domain of HuGnTI performs less in plants than the plant catalytic domain.

Materials and methods

Plant materials and growth conditions

Seeds of *Arabidopsis thaliana* lines were sown on 9 cm 0.8% daishun agar Petri dishes and placed in a cold room at 4°C for 2 days in the dark to promote uniform germination. Plants were grown in soil in a greenhouse with a 16 h day/8 h dark cycle at a temperature of 22°C.

Construction of GFP/CFP-tagged GnTI vectors

Arabidopsis and human GnTI was PCR amplified using Platinum Pfx polymerase (Invitrogen) and primers flanking the coding region. The primers used for cloning the AtGnTI were AtGnT-F (5'-GTGACA-GATCTATGGCGAGGATCTCGTGACTT G-3') and AtGnT-R (5'-GTGACCCCATGGAATTCGAAT TCCAAGCTGC-3') which contain a *Bgl*II and *Nco*I site respectively, with the *Nco*I site deleting the original stop codon. The primers used for cloning the HuGnTI were FW13 HuGnT (5'-GTGACGGTCTC AGATCTATGCTGAAGAACAGTCTGCA-3') and

RV10 HuGnT (5'- GTGACGGTCTCACATGCGAT TCCAGCTAGGATCAT-3' which both contain a *Bsa*I site that after digest leave a *Bgl*II and *Nco*I overhang respectively, with the *Nco*I site deleting the original stop codon. The full-length GnTIs cDNA was inserted into the *Bgl*II and *Nco*I site of the pMON999-CFP/YFP (Monsanto, St. Louis, MO) transfection vector.

Construction of chimeric plant/human GnTI

A chimeric construct of GnTI was generated by fusing the *Arabidopsis* GnTI CTS domain (amino acid 1–102) and the mammalian GnTI catalytic domain (amino acid 102–445). The putative CTS region of *Arabidopsis* was amplified by PCR using Platinum pfx Polymerase (Invitrogen) with the primers AtGnTI CTS-F (5'GGTCTCAGATCTATGGCGA GGATCTCGT GTGACTTG-3') and AtGnTI CTS-R (5'-AACTCACTCAAGGTGGACAGGCGGTGAT T-3'). The fragment encoding the catalytic domain of the human GnTI was amplified using the primers HuGnTI cat-F (5'-GGTGGACAGGCGGTGATTCC-CATCCTGG-3') and RV10 HuGnTI (5'- GTGAC GGTCTCACATGCGATTCCAGCTAGGATCAT-3'). The AthGNTI CTS-R primer and the HU-CAT primer were overlapping in the sequence 5'-GGTGGACAG GCGGTGATT-3'. The PCR products were purified using the QIAquick PCR Purification Kit (Qiagen). The CTS domain and the human catalytic domain were hybridized together using the PCR products as megaprimer in a second PCR, together with the AtGnT CTS-F and RV10 HuGnT primers for the generation of the full length chimeric GnTI. The sequence of the fusion product was verified by DNA sequencing of the cloned PCR product and the full-length ChGnTI cDNA was inserted into the *Bgl*II and *Nco*I site of pMON999-CFP/YFP (Monsanto, St. Louis, MO) transfection vector.

Construction of the binary vectors

The pMON vectors with the AtGnTI-YFP and ChGnTI-YFP constructs were digested by HindIII and SmaI, and the resulting 35S-GnTI-YFP DNA fragments were isolated and ligated into the HindIII and SmaI sites of the pBin⁺ vector. For construction of the HuGnTI expression vector, the pMON vector of the HuGnTI-YFP construct was cut by Hind III and Sca I in order to isolate the 35S promoter-

HuGnTI CTS domain DNA fragment. This fragment was used to replace the 35S promoter-AtGnTI CTS domain in the pBin⁺ with ChGnTI-YFP.

Transformation of *Arabidopsis*

pBinplus constructs containing the GnTI-YFP cassettes were transferred to *Agrobacterium tumefaciens* AGL-0 by triparental mating using the *E.Coli* pRK2013 helper plasmid. *Arabidopsis* plants were transformed by immersion in the bacteria suspension culture. Seeds from transformed plants were selected by growing on plates containing MS powder (4.4 g/l), sucrose (10 g/l) and Daishin agar (8 g/l) with kanamycin (50 µg/ml) as selective marker. Seeds were germinated and grown on selective medium for 1–2 weeks (25°C long day conditions). The putative transformants were transferred to soil and grown using standard conditions (16 h day/8 h dark).

Arabidopsis protoplast isolation and transfection

Arabidopsis mesophyll protoplasts were prepared and transfected according to Aker et al. (2006). Protoplasts were investigated for CFP/YFP expression with a confocal laser scanning microscope 510 as described before (Shah et al. 2002) (Carl Zeiss, Jena, Germany).

SDS-PAGE and immunoblotting

Plant material was ground in liquid nitrogen, resuspended in 10 µl phosphate-buffered saline (137 mM NaCl, 2.7 mM KCl, 10 mM Na₂HPO₄, 2 mM KH₂PO₄, pH 7.4) per mg of plant material and centrifuged. The protein concentration of each sample was measured using the Bio-Rad RC/DC protein assay using the manufacturer's instructions and 5 µg of total protein from each sample was mixed with SDS-polyacrylamide gel electrophoresis (PAGE) loading buffer, denatured at 95°C for 5 min and subjected to SDS-PAGE (8 or 12.5%) under reducing conditions. Western blotting was performed using PVDF membranes, blocked with 5% (w/v) non-fat dry milk in Tris-buffered saline (TBS, 20 mM Tris-HCl, pH 7.6, 137 mM NaCl) with 0.05% Tween20. The membranes were probed with either anti-HRP (1:2000; Sigma) or anti-GFP (1:5000; Roche). Detection of bound primary antibodies was performed with

BCIP/NBT or after incubation with goat anti-rabbit antibodies.

Elisa

Microtiter plates were coated with equal amounts of total protein extracts from transformed *cgl1-1* seedlings overnight at 4°C in 0.1 M sodium carbonate buffer, pH 9.6. The plates were washed with phosphate-buffered saline (PBS) containing 0.05% Tween 20 and blocked with PBS-T containing 5% skimmed milk for 1 h at RT. After the washing the plates were incubated for 1 h at RT with anti-HRP diluted 1:2,000. Detection of bound primary antibodies was performed with AP substrate after incubation with goat anti-rabbit antibodies.

RNA isolation and RT-PCR analysis

RNA was extracted from transformed *cgl1-1* seedlings using TriPure isolation reagent (Roche) and the concentration was measured with a NanoDrop® ND-1000 UV-Vis Spectrophotometer. 1 µg of RNA was used to make cDNA with Taqman Reverse Transcript reagent (Applied Biosystems). Quantitative real-time PCR was performed using the Bio-Rad iQSYBR Green Supermix single color detection system. Briefly, after a 3 min denaturation at 94°C, 40 cycles of 15 s at 94°C and 30 s at 60°C were followed by a melting curve gradient. No template controls served as blanks and β-Actin was used as a reference gene. Samples were run in triplicate, averaged, and relative gene expression was calculated using the $2^{-\Delta\Delta t}$ method (Livak and Schmittgen 2001). Primers were designed using Beacon Designer (Biosoft International, Palo Alto, USA) and ordered by Invitrogen. The primer pair YFP-F (5'-TTCAAGGAGGACGGCAAC-3') and YFP-R (5'-GG TGTTCTGCTGGTAGTG-3') was used for the experiment.

Open Access This article is distributed under the terms of the Creative Commons Attribution Noncommercial License which permits any noncommercial use, distribution, and reproduction in any medium, provided the original author(s) and source are credited.

References

- Aker J, Borst JW, Karlova R, de Vries S (2006) The *Arabidopsis thaliana* AAA protein CDC48A interacts in vivo with the somatic embryogenesis receptor-like kinase 1 receptor at the plasma membrane. *J Struct Biol* 156:62–71
- Bakker H, Bardor M, Molthoff JW, Gomord V, Elbers I, Stevens LH, Jordi W, Lommen A, Faye L, Lerouge P, Bosch D (2001) Galactose-extended glycans of antibodies produced by transgenic plants. *Proc Natl Acad Sci USA* 98:2899–2904
- Brandizzi F, Frangne N, Marc-Martin S, Hawes C, Neuhaus JM, Paris N (2002) The destination for single-pass membrane proteins is influenced markedly by the length of the hydrophobic domain. *Plant Cell* 14:1077–1092
- Burke J, Pettitt JM, Humphris D, Gleeson PA (1994) Medial-Golgi retention of *N*-acetylglucosaminyltransferase I. Contribution from all domains of the enzyme. *J Biol Chem* 269:12049–12059
- Clough SJ, Bent AF (1998) Floral dip: a simplified method for Agrobacterium-mediated transformation of *Arabidopsis thaliana*. *Plant J* 16:735–743
- Fukada T, Iida K, Kioka N, Sakai H, Komano T (1994) Cloning of a cDNA encoding *N*-acetylglucosaminyltransferase I from rat liver and analysis of its expression in rat tissues. *Biosci Biotechnol Biochem* 58:200–201
- Gomez L, Chrispeels MJ (1994) Complementation of an *Arabidopsis thaliana* mutant that lacks complex asparagine-linked glycans with the human cDNA encoding *N*-acetylglucosaminyltransferase I. *Proc Natl Acad Sci USA* 91:1829–1833
- Grabenhorst E, Conradt HS (1999) The cytoplasmic, transmembrane, and stem regions of glycosyltransferases specify their in vivo functional sublocalization and stability in the Golgi. *J Biol Chem* 274:36107–36116
- Grebe M, Xu J, Möbius W, Ueda T, Nakano A, Geuze HJ, Rook MB, Scheres B (2003) *Arabidopsis* sterol endocytosis involves actin-mediated trafficking via ARA6-positive early endosomes. *Curr Biol* 13:1378–1387
- Helenius J, Aeby M (2002) Transmembrane movement of dolichol linked carbohydrates during N-glycoprotein biosynthesis in the endoplasmic reticulum. *Semin Cell Dev Biol* 13:171–178
- Kornfeld R, Kornfeld S (1985) Assembly of asparagine-linked oligosaccharides. *Annu Rev Biochem* 54:631–664
- Kumar R, Yang J, Larsen RD, Stanley P (1990) Cloning and expression of *N*-acetylglucosaminyltransferase I, the medial Golgi transferase that initiates complex N-linked carbohydrate formation. *Proc Natl Acad Sci USA* 87:9948–9952
- Lisenbee CS, Karnik SK, Trelease RN (2003) Overexpression and mislocalization of a tail-anchored GFP redefines the identity of peroxisomal ER. *Traffic* 4:491–501
- Livak KJ, Schmittgen TD (2001) Analysis of relative gene expression data using real-time quantitative PCR and the 2(-Delta Delta C(T)) Method. *Methods* 25:402–408
- Masclaux FG, Galaud JP, Pont-Lezica R (2005) The riddle of the plant vacuolar sorting receptors. *Protoplasma* 226:103–108
- Neumann U, Brandizzi F, Hawes C (2003) Protein transport in plant cells: in and out of the Golgi. *Ann Bot (Lond)* 92:167–180
- Palacpac NQ, Yoshida S, Sakai H, Kimura Y, Fujiyama K, Yoshida T, Seki T (1999) Stable expression of human beta1, 4-galactosyltransferase in plant cells modifies N-

- linked glycosylation patterns. Proc Natl Acad Sci USA 96:4692–4697
- Pownall S, Kozak CA, Schappert K, Sarkar M, Hull E, Schachter H, Marth JD (1992) Molecular cloning and characterization of the mouse UDP-*N*-acetylglucosamine:alpha-3-D-mannoside beta-1, 2-*N*-acetylglucosaminyltransferase I gene. Genomics 12:699–704
- Puthalakath H, Burke J, Gleeson PA (1996) Glycosylation defect in Lec1 Chinese hamster ovary mutant is due to a point mutation in *N*-acetylglucosaminyltransferase I gene. J Biol Chem 271:27818–27822
- Saint-Jore-Dupas C, Nebenfuhr A, Boulaflous A, Follet-Gueye ML, Plasson C, Hawes C, Driouich A, Faye L, Gomord V (2006) Plant *N*-glycan processing enzymes employ different targeting mechanisms for their spatial arrangement along the secretory pathway. Plant Cell 18:3182–3200
- Sarkar M, Hull E, Nishikawa Y, Simpson RJ, Moritz RL, Dunn R, Schachter H (1991) Molecular cloning and expression of cDNA encoding the enzyme that controls conversion of high-mannose to hybrid and complex *N*-glycans: UDP-*N*-acetylglucosamine: alpha-3-D-mannoside beta-1, 2-*N*-acetylglucosaminyltransferase I. Proc Natl Acad Sci USA 88:234–238
- Schachter H, Chen SH, Zhou S, Tan J, Yip B, Sarkar M, Spence A (1997) Structure and function of the genes encoding *N*-acetylglucosaminyltransferases which initiate *N*-glycan antennae. Biochem Soc Trans 25:875–880
- Shah K, Russinova E, Gadella TW Jr, Willemse J, De Vries SC (2002) The Arabidopsis kinase-associated protein phosphatase controls internalization of the somatic embryogenesis receptor kinase 1. Genes Dev 16:1707–1720
- Snider MD, Sultzman LA, Robbins PW (1980) Transmembrane location of oligosaccharide-lipid synthesis in microsomal Golgi stacks. Cell 21:385–392
- Strasser R, Steinkellner H, Boren M, Altmann F, Mach L, Glossl J, Mucha J (1999) Molecular cloning of cDNA encoding *N*-acetylglucosaminyltransferase II from *Arabidopsis thaliana*. Glycoconj J 16:787–791
- Strasser R, Stadlmann J, Svoboda B, Altmann F, Glossl J, Mach L (2005) Molecular basis of *N*-acetylglucosaminyltransferase I deficiency in *Arabidopsis thaliana* plants lacking complex *N*-glycans. Biochem J 387:385–391
- Tusnady GE, Simon I (2001) The HMMTOP transmembrane topology prediction server. Bioinformatics 17:849–850
- van Engelen FA, Molthoff JW, Conner AJ, Nap JP, Pereira A, Stiekema WJ (1995) pBINPLUS: an improved plant transformation vector based on pBIN19. Transgenic Res 4:288–290
- von Schaewen A, Sturm A, O'Neill J, Chrispeels MJ (1993) Isolation of a mutant *Arabidopsis* plant that lacks *N*-acetyl glucosaminyl transferase I and is unable to synthesize Golgi-modified complex *N*-linked glycans. Plant Physiol 102:1109–1118
- Wenderoth I, von Schaewen A (2000) Isolation and characterization of plant *N*-acetyl glucosaminyltransferase I (GntI) cDNA sequences. Functional analyses in the *Arabidopsis* cgl mutant and in antisense plants. Plant Physiol 123:1097–1108
- Yoshida S, Suzuki M, Yamano S, Takeuchi M, Ikenaga H, Kioka N, Sakai H, Komano T (1999) Expression and characterization of rat UDP-*N*-acetylglucosamine: alpha-3-D-mannoside beta-1, 2-*N*-acetylglucosaminyltransferase I in *Saccharomyces cerevisiae*. Glycobiology 9:53–58